Theoretical and Experimental Studies of the Diels−Alder Dimerizations of Substituted Cyclopentadienes

Robert D. J. Froese,[†] Michael G. Organ,[‡,⊥] John D. Goddard,*[,†] T. Daniel P. Stack,[‡] and Barry M. Trost*[,‡]

Contribution from the Guelph-Waterloo Centre for Graduate Work in Chemistry, Department of Chemistry and Biochemistry, University of Guelph, Guelph, Ontario N1G 2W1, and Department of Chemistry, Stanford University, Stanford, California 94035-5080

Received May 24, 1995. Revised Manuscript Received September 1, 1995[⊗]

Abstract: Diels−Alder dimerizations of a series of substituted cyclopentadienes have been studied. Experimentally, preparation of 1-oxaspiro[2.4]hepta-4,6-diene results in immediate formation of the Diels−Alder dimer with two adducts formed in a ratio of 3:1. Two substituted spiroheptadiene systems gave similar results. Theoretically, transition states for four different isomers were located leading to the four dimer minima of 1-oxaspiro[2.4]hepta-4,6-diene. The transition state associated with the lowest of the four energetic barriers leads to the isomer with the same connectivity as the major isomer obtained in the dimerization of 2,2-dimethyl-1-oxaspiro[2.4]hepta-4,6-diene (structure confirmed by X-ray diffraction analysis). Unsymmetric transition states at the HF/6-31G(d) level were predicted for three additional *endo* species with the energy barriers decreasing in the following order: spiro[2.4]hepta-4,6-diene > cyclopentadiene > 1-oxaspiro[2.4]hepta-4,6-diene > 1,2-dioxaspiro[2.4]hepta-4,6-diene. The barrier to forming the dimer of spiro[2.4]hepta-4,6-diene is predicted to be approximately 5 kcal/mol greater than that for forming the cyclopentadiene dimer and about 13 kcal/mol greater than the barrier to formation of the dimer of 1-oxaspiro[2.4]-hepta-4,6-diene.

Introduction

Diels−Alder reactions[1] have been studied in great detail both theoretically and experimentally. Experimentally, it has been shown that the process is concerted.[2] Although the reactions are usually quite exothermic, early transition states are not always indicated as would be expected on the basis of Hammond's postulate.[3] Synchronous transition states have been predicted theoretically for the prototypal 1,4-addition of ethylene to butadiene, e.g. ref 4. However, for unsymmetrical reactants, the transition states must be more or less asynchronous, and the two bonds which are being formed often can differ distinctly in their lengths. There is both experimental[5] and theoretical[6−8] evidence for the asynchronicity of such transition states. A number of semiempirical[7,9−23] and *ab initio*[24−30] theoretical studies of Diels−Alder cycloadditions have been conducted. Some studies[4] have shown that *ab initio* SCF methods favor a concerted mechanism[5] which was usually invoked by experimentalists, while semiempirical approaches favor steps involving biradicals. In addition, there have been several recent reviews[31,32] on the modeling of transition states and on stereoselectivity.

Various explanations have been proposed for the selectivities observed in these reactions. Orbital tilting of the diene was suggested to lead to the facial selectivity of isodicyclopentadi-

* To whom correspondence should be sent.
† University of Guelph.
‡ Stanford University.
§ Current address: Department of Chemistry, Indiana University−Purdue University at Indianapolis, 402 N. Blackford St., Indianapolis, Indiana 46202-3274.
⊗ Abstract published in *Advance ACS Abstracts,* October 15, 1995.

(1) Diels, O.; Alder, K. *Justus Liebigs Ann. Chem.* **1928**, *460*, 98.
(2) Sauer, J.; Sustmann, R. *Angew. Chem., Int. Ed. Engl.* **1980**, *19*, 779.
(3) Hammond, G. S. *J. Am. Chem. Soc.* **1955**, *77*, 334.
(4) Brown, F. K.; Houk, K. N. *Tetrahedron Lett.* **1984**, *25*, 4609.
(5) Gajewski, J. J.; Peterson, K. B.; Kagel, J. R. *J. Am. Chem. Soc.* **1987**, *109*, 5545.
(6) (a) Brown, F. K.; Houk, K. N.; Burnell, D. J.; Valenta, Z. *J. Org. Chem.* **1987**, *52*, 3050. (b) Brown, F. K.; Houk, K. N. *Tetrahedron Lett.* **1985**, *26*, 2297.
(7) Loncharich, R. J.; Brown, F. K.; Houk, K. N. *J. Org. Chem.* **1989**, *54*, 1129.
(8) Woodward, R. B.; Katz, T. J. *Tetrahedron* **1959**, *5*, 70.
(9) Basilevsky, M. V.; Tikhomirov, V. A.; Chlenov, I. E. *Theor. Chim. Acta* **1971**, *23*, 75.
(10) Kikuchi, O. *Tetrahedron* **1971**, *27*, 2791.
(11) McIver, J. W., Jr. *Acc. Chem. Res.* **1974**, *7*, 72.
(12) Dewar, M. J. S.; Griffin, A. C.; Kirschner, S. *J. Am. Chem. Soc.* **1974**, *96*, 6225.
(13) Basilevsky, M. V.; Shamov, A. G.; Tikhomirov, V. A. *J. Am. Chem. Soc.* **1977**, *99*, 1369.
(14) Dewar, M. J. S.; Olivella, S.; Rzepa, H. S. *J. Am. Chem. Soc.* **1978**, *100*, 5650.
(15) Jug, K.; Krüger, H.-W. *Theor. Chim. Acta* **1979**, *52*, 19.
(16) Pancfr, J. *J. Am. Chem. Soc.* **1982**, *104*, 7424.
(17) Dewar, M. J. S.; Pierini, A. B. *J. Am. Chem. Soc.* **1984**, *106*, 203.
(18) Dewar, M. J. S. *J. Am. Chem. Soc.* **1984**, *106*, 209.
(19) Dewar, M. J. S.; Olivella, S.; Stewart, J. J. P. *J. Am. Chem. Soc.* **1986**, *108*, 5771.
(20) Dewar, M. J. S.; Zoebisch, E. G.; Healy, E. F.; Stewart, J. J. P. *J. Am. Chem. Soc.* **1985**, *107*, 3902.
(21) Doi, T.; Shimizu, K.; Takahashi, T.; Tsuji, J.; Yamamoto, K. *Tetrahedron Lett.* **1990**, *31*, 3313.
(22) Takahashi, T.; Sakamoto, Y.; Doi, T. *Tetrahdron Lett.* **1992**, *33*, 3519.
(23) Marshall, J. A.; Grote, J.; Audia, J. E. *J. Am. Chem. Soc.* **1987**, *109*, 1186.
(24) Burke, L. A.; Leroy, G.; Sana, M. *Theor. Chim. Acta* **1975**, *40*, 313.
(25) Townshend, R. E.; Ramunni, G.; Segal, G.; Hehre, W. J.; Salem, L. *J. Am. Chem. Soc.* **1976**, *98*, 2190.
(26) Burke, L. A.; Leroy, G. *Theor. Chim. Acta* **1977**, *44*, 219.
(27) Ortega, M.; Oliva, A.; Lluch, J. M.; Bertran, J. *Chem. Phys. Lett.* **1983**, *102*, 317.
(28) Bernardi, F.; Bottoni, A.; Robb, M. A.; Field, M. J.; Hillier, I. H.; Guest, M. F. *J. Chem. Soc., Chem. Commun.* **1985**, 1051.
(29) Burke, L. A. *Int. J. Quantum Chem.* **1986**, *29*, 511.
(30) Houk, K. N.; Lin, Y.-T.; Brown, F. K. *J. Am. Chem. Soc.* **1986**, *108*, 554.
(31) Eksterowicz, J. E.; Houk, K. N. *Chem. Rev.* **1993**, *93*, 2439.
(32) Houk, K. N.; Paddon-Row, M. N.; Rondan, N. G.; Wu, Y.-D.; Brown, F. K.; Spellmeyer, D. C.; Metz, J. T.; Li, Y.; Loncharich, R. J. *Science* **1986**, *231*, 1108.

0002-7863/95/1517-10931$09.00/0

ene.[33] It has been proposed that in certain cyclopentadienes, the stereoselectivity arises from torsional effects in the cyclopentadiene framework, which can be overridden by steric effects due to substituents.[6,34] Secondary orbital interactions[35] have been considered important as a rationale for the observation of *endo* rather than *exo* products. Recently, HOMO/LUMO gaps in 5,5-disubstituted cyclopentadienes have been examined and correlated with Diels–Alder reactivity.[36] The concept of "spiroconjugation" was invoked by these authors to explain the tendency for such compounds to dimerize. There also were a number of earlier experiments involving cyclopentadienes with oxygen substituents, and these compounds were found to dimerize.[37]

From a synthetic viewpoint, substituted cyclopentadienes are very important compounds. Our specific interest in 1-oxaspiro[2.4]hepta-4,6-diene lay in its potential use as a substrate in Pd(0) catalyzed addition and substitution reactions involving a vinyl epoxide in the presence of the second double bond in the cyclopentadiene derivative. The development of such synthetic methodology would be of great use in the preparation of highly-functionalized 5-membered ring compounds. Experimentally, both the preparation of and dimerization of 1-oxaspiro[2.4]hepta-4,6-diene will be examined.

This work also presents a theoretical study of the dimerization of cyclopentadiene and of three spiroheptadienes derived from cyclopentadiene. Experimentally, spiro[2.4]hepta-4,6-diene does not dimerize and is sufficiently stable so as to be available commercially. Cyclopentadiene will dimerize albeit slowly, 1-oxaspiro[2.4]hepta-4,6-diene dimerizes rapidly, and 1,2-dioxaspiro[2.4]hepta-4,6-diene is unstable.[38] This research considers a true dimerization, thus the diene and the dienophile are identical. Examination of the highest occupied molecular orbitals (HOMO) and the lowest unoccupied molecular orbitals (LUMO) of the four species of interest gives insight into the reactions.

Ab initio theoretical methods were used with full geometry optimizations at the 6-31G(d) SCF level for the following (all transition states and dimers are *endo* except where noted): cyclopentadiene monomer (**1**), *endo* dimer (**2**), *endo* transition state (**3**), *exo* dimer (**4**), and *exo* transition state (**5**); the spiro[2.4]hepta-4,6-diene monomer (**6**), dimer (**7**), and transition state (**8**); the 1,2-dioxaspiro[2.4]hepta-4,6-diene monomer (**9**), dimer (**10**), and transition state (**11**); the four possible 1-oxaspiro[2.4]-hepta-4,6-diene compounds, monomer **12**, dimers **13**–**16**, and the corresponding transition states **17**–**20**. Figures 1 to 4 illustrate many of these species.

Discussion

Experimental Results. In developing a general approach to highly-functionalized five-membered-ring-containing natural products, we envisioned the use of a class of substituted cyclopentadiene compounds with the general structure of **12** (see Figure 1). It is known that vinyl epoxides are suitable substrates for Pd catalyzed epoxide ring openings in order to generate π-allyl palladium cation intermediates that can react with a variety of nucleophiles.[39] Such a reaction would be a novel one with **12**, as one could generate, stabilize, and alkylate

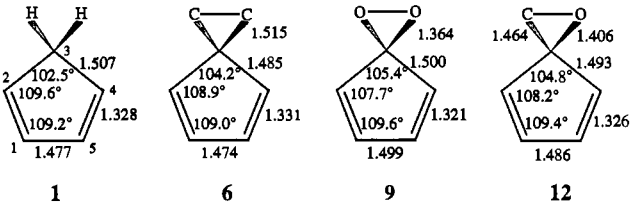

1 **6** **9** **12**

Figure 1. The geometries of the monomers of cyclopentadiene and of spiroheptadienes: the species depicted above are cyclopentadiene (**1**), spiro[2.4]hepta-4,6-diene (**6**), 1,2-dioxaspiro[2.4]hepta-4,6-diene (**9**), and 1-oxaspiro[2.4]hepta-4,6-diene (**12**). The numbering scheme for the monomers is indicated on cyclopentadiene. The experimental values for cyclopentadiene (ref 50) are the following: bond lengths C_3-C_4 1.506 Å, C_4-C_5 1.345 Å, and C_1-C_5 1.468 Å; bond angles $C_2-C_3-C_4$ 102.9°, $C_1-C_2-C_3$ 109.2°, and $C_2-C_1-C_5$: 109.3°.

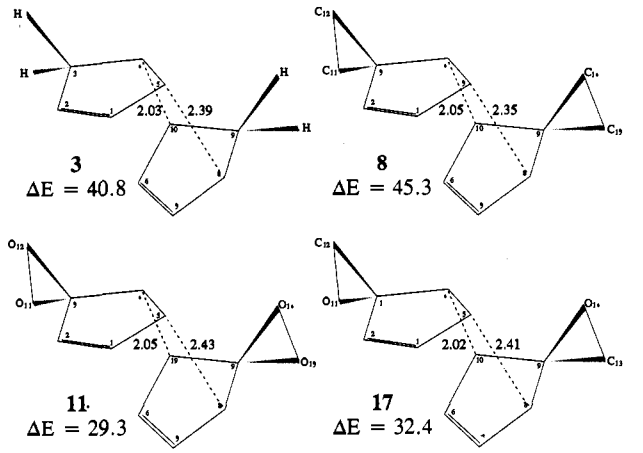

Figure 2. The structure of the *endo* transition states for cyclopentadiene and the substituted cyclopentadiene systems. The systems include the cyclopentadiene transition state (**3**), the spiro[2.4]hepta-4,6-diene transition state (**8**), the 1,2-dioxaspiro[2.4]hepta-4,6-diene transition state (**11**), and one of the 1-oxaspiro[2.4]hepta-4,6-diene transition states (**17**). The lengths of the carbon–carbon bonds which are forming in the transition state are shown. The relative energies (kcal/mol) with respect to two isolated monomers are given.

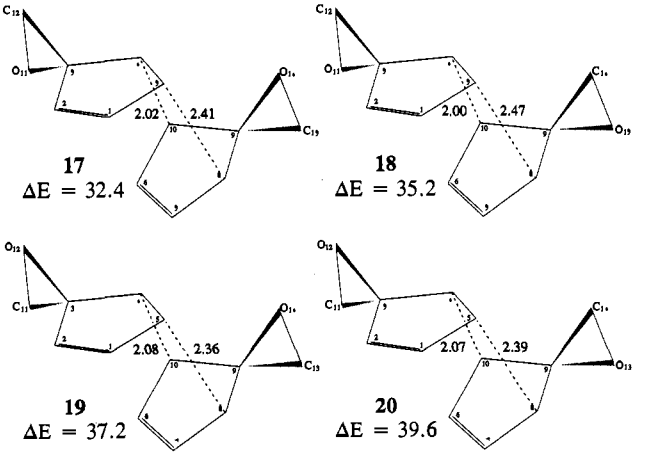

Figure 3. The structures of the four *endo* transition states for the dimerization of 1-oxaspiro[2.4]hepta-4,6-diene. The lengths of the carbon–carbon bonds which are forming in these transition states are shown. The relative energies (kcal/mol) with respect to two isolated monomers are given.

(33) Gleiter, R.; Paquette, L. A. *Acc. Chem. Res.* **1983**, *16*, 328.
(34) Brown, F. K.; Houk, K. N. *J. Am. Chem. Soc.* **1985**, *107*, 1971.
(35) (a) Houk, K. N.; Strozier, R. W. *J. Am. Chem. Soc.* **1973**, *95*, 4094. (b) Alston, P. V.; Ottenbrite, R. M.; Shillady, D. D. *J. Org. Chem.* **1973**, *38*, 4075. (c) Alston, P. V.; Ottenbrite, R. M.; Cohen, T. *J. Org. Chem.* **1978**, *43*, 1864. (d) Cohen, T.; Ruffner, R. J.; Shull, D. W.; Daniewski, W. M.; Ottenbrite, R. M.; Alston, P. V. *J. Org. Chem.* **1978**, *43*, 4052. (e) Hoffmann, R.; Woodward, R. B. *J. Am. Chem. Soc.* **1965**, *87*, 4388.
(36) Raman, J. V.; Nielsen, K. E.; Randall, L. H.; Burke, L. A.; Dmitrienko, G. I. *Tetrahedron Lett.* **1994**, *35*, 5973.
(37) (a) Depuy, C. H.; Isaks, M.; Eilers, K. L.; Morris, G. F. *J. Org. Chem.* **1964**, *29*, 3503. (b) Depuy, C. H.; Ponder, B. W.; Fitzpatrick, J. D. *J. Org. Chem.* **1964**, *29*, 3508.
(38) (a) Dunkin, I. R.; Shields, C. J. *J. Chem. Soc., Chem. Commun.* **1986**, 154. (b) Bell, G. A.; Dunkin, I. R.; Shields, C. J. *Spectrochim. Acta, Part A* **1985**, *41*, 1221. (c) Chapman, O. L.; Hess, T. C. *J. Am. Chem. Soc.* **1984**, *106*, 1842. (d) Chapman, O. L.; Hess, T. C. *J. Org. Chem.* **1979**, *44*, 962.

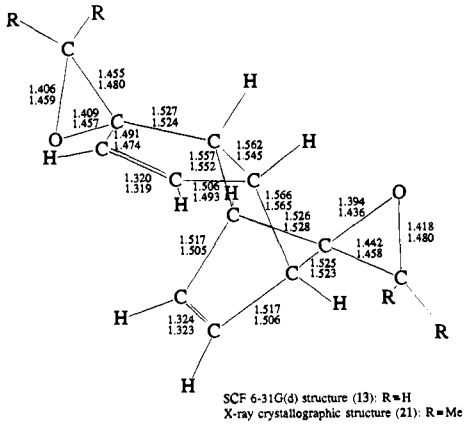

Figure 4. Key bond lengths for the lowest energy dimer of 1-oxaspiro-[2.4]hepta-4,6-diene (**13**) (R = H). The dimer was optimized fully at the Hartree–Fock level of theory using the 6-31G(d) basis set. The geometry of the X-ray crystallographic structure of the substituted adduct (R = Me) (**21**) is also given.

Scheme 1

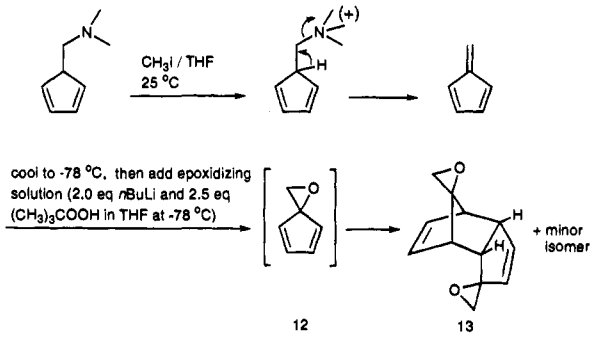

a formally antiaromatic cationic species. Moreover, the product of such an addition is still a diene and thus suitable for many subsequent transformations, such as [4 + 2] cycloadditions.

It was on route to preparing **12** that we discovered the strong tendency for molecules of this general type to dimerize once formed. The formation of the antiaromatic Pd cation intermediate has been achieved using different substrates, and that work is continuing. The initial observations of dimerization lead us to a wider study not only to obtain a suitable epoxide substrate but also to gain further understanding of the features which control such dimerization reactions.

After much initial experimentation to generate and epoxidize fulvene, the optimized sequence shown in Scheme 1 was used. Owing to the low boiling point and lack of polarity, fulvene itself is difficult to isolate, so it was prepared as a solution in THF and epoxidized directly using the Meth-Cohn procedure.[40] The structure of **13** (see Figure 3) was assessed by comparison of its spectral data with that of **21** (see Scheme 2), for which X-ray crystal structure analysis had been used to determine its connectivity. Analysis of proton NMR spectra of crude samples taken from the reaction mixture during epoxidation revealed only unepoxidized fulvene and dimer. Similar analyses were performed during the epoxidation of compounds **23** and **24** shown in Scheme 2. Although we never spotted any monomer during such analyses, we cannot state for certain that dimerization occurred at −78 °C as monomer was formed, or while the sample warmed. Nonetheless, the monomers in this series have a very brief existence.

(39) (a) Trost, B. M. *Angew. Chem., Int. Ed. Engl.* **1989**, *28*, 1173. (b) Trost, B. M.; Ito, N.; Greenspan, P. D. *Tetrahedron Lett.* **1993**, *34*, 1421.

(40) Meth-Cohn, O.; Moore, C.; Taljaard, H. C. *J. Chem. Soc., Perkin Trans. 1* **1988**, 2663.

Scheme 2

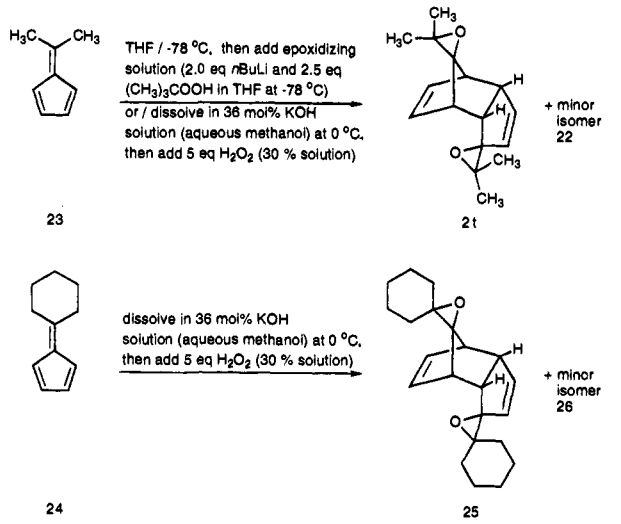

6,6-Dimethylfulvene (**23** in Scheme 2)[41a] had been epoxidized previously by Alder who reported **21** as the sole product when epoxidation was carried out using H_2O_2 in MeOH/H_2O.[41b] In that case, the product was isolated via crystallization from the reaction mixture by adding additional H_2O when epoxidation was judged complete. In the current study, we repeated this experiment with the exception that the reaction was followed by a reductive workup and extraction into ether. It turns out that **22** is also a product as the minor isomer in a ratio of 3:1 using Alder's conditions. The identical product ratio was obtained using Meth-Cohn conditions.

Compound **24**[41a] was epoxidized using the same H_2O_2 conditions as above in the epoxidation of **23** and a 2:1 ratio of **25** to **26** was obtained. The structure of **25** was determined by analysis of its spectra and through comparison with **21**. See Scheme 2 for the structures of these compounds. The structures of the minor isomers were not conclusively determined.

Competition experiments have been conducted in the past[42] and it was found that the methyl, ethyl, and trimethylene ketals of cyclopentadienone could routinely be trapped with good dienophiles such as maleic anhydride, benzoquinone, and acrolein. Interestingly, in some studies, the ethylene ketal of cyclopentadienone could not be trapped and only dimer was obtained. Obviously, the cyclic nature of these oxygen-containing spirobicyclocyclopentadienes is involved in their tendency to dimerize, rather than to form cross adducts.

Theoretical Results. (a) Energetics. *Ab initio* theoretical studies with full geometry optimizations at the 6-31G(d) SCF level were performed. All species considered arising from the dimerization were *endo* except for cyclopentadiene itself where the *exo* addition was also examined for comparison. The *endo* and *exo* cyclopentadiene transition states have been studied recently by Jorgenson[43] at similar levels of theory and those results are verified here.

The energetic data for the monomers, dimers, and transition states are collected in Table 1. Many of the structures are depicted in Figures 1–3. Figure 4 gives key geometrical predictions for the lowest energy adduct of 1-oxaspiro[2.4]hepta-4,6-diene. Figure 5 presents similar geometrical detail for the transition state structure. Note the unconventional numbering

(41) (a) Collins, S.; Hong, Y.; Kataoka, M.; Nguyen, T. *J. Org. Chem.* **1990**, *55*, 3395. (b) Alder, K.; Flock, F. H.; Lessenich, H. *Chem. Ber.* **1957**, *90*, 1709.

(42) (a) Barborak, J. C.; Pettit, R. *J. Am. Chem. Soc.* **1967**, *89*, 3080. (b) Eaton, P. E.; Hudson, R. A. *J. Am. Chem. Soc.* **1965**, *87*, 2769.

(43) Jorgensen, W. L.; Lim, D.; Blake, J. F. *J. Am. Chem. Soc.* **1993**, *115*, 2936.

Table 1. Energetic Data on the Monomer, *Endo* Transition State, and *Endo* Dimer for the Three Substituted Cyclopentadienes, Spiro[2.4]hepta-4,6-diene (**6**–**8**), 1,2-Dioxaspiro[2.4]hepta-4,6-diene (**9**–**11**), and 1-Oxaspiro[2.4]hepta-4,6-diene (**12**–**20**). Energies for Cyclopentadiene, the *Endo* (**2**) and *Exo* (**4**) Dimer Products and the Transition States (**3** and **5**); SCF Level Energies for the Fully Optimized Geometries Using the 6-31G(d) Basis Set

compd[a]	total energy (au)	molecule	ΔE[b]
	Cyclopentadiene Dimer ($C_{10}H_{12}$)		
1	−192.791 721	monomer	
1/1	−385.583 442	two monomers	0.0
2	−385.612 768	dimer	−18.4
3	−385.518 435	TS	40.8
4	−385.614 716	dimer	−19.6
5	−385.514 362	TS	43.3
	Spiro[2.4]hepta-4,6-diene Dimer ($C_{14}H_{16}$)		
6	−269.663 174	monomer	
6/6	−539.326 348	two monomers	0.0
7	−539.346 776	dimer	−12.8
8	−539.254 155	TS	45.3
	1,2-Dioxaspiro[2.4]hepta-4,6-diene Dimer ($C_{10}H_8O_4$)		
9	−341.212 565	monomer	
9/9	−682.425 130	two monomers	0.0
10	−682.478 672	dimer	−33.6
11	−682.378 436	TS	29.3
	1-Oxaspiro[2.4]hepta-4,6-diene dimer ($C_{12}H_{12}O_2$)		
12	−305.471 539	monomer	
12/12	−610.943 078	two monomers	0.0
13	−610.985 130	dimer	−26.4
14	−610.983 880	dimer	−25.6
15	−610.981 366	dimer	−24.0
16	−610.981 195	dimer	−23.9
17	−610.891 490	TS	32.4
18	−610.886 916	TS	35.2
19	−610.883 821	TS	37.2
20	−610.879 956	TS	39.6

[a] See Figures 1–4 for the structures of the molecules. [b] ΔE (kcal/mol) is the energy difference between the dimer and two infinitely separated monomers.

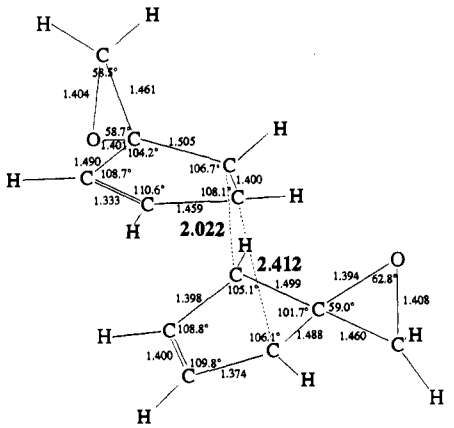

Figure 5. Key bond lengths and bond angles of the transition state for the dimerization of the lowest energy 1-oxaspiro[2.4]hepta-4,6-diene (**17**) species. This transition state was optimized fully at the Hartree–Fock level, using the 6-31G(d) basis set. The dashed lines indicate the major components of the reaction coordinate at the transition state, which are the two carbon–carbon bonds being formed. These bond lengths are 2.022 and 2.412 Å.

scheme for the atoms in the compounds given in Figures 1–3 which will be used to ease comparison between monomers, transition states, and dimers/cycloadducts.

Transition state barriers measured relative to reactants are predicted to be 40.8 kcal/mol (**3**-*endo*) or 43.3 kcal/mol (**5**-*exo*) for cyclopentadiene, 45.3 kcal/mol for spiro[2.4]hepta-4,6-diene (**8**), 29.3 kcal/mol for 1,2-dioxaspiro[2.4]hepta-4,6-diene (**11**), and 32.4 (**17**), 35.2 (**18**), 37.2 (**19**), and 39.6 kcal/mol (**20**) for the four different 1-oxaspiro[2.4]hepta-4,6-diene adducts. Experimentally, cyclopentadiene dimerization leads only to the *endo* product.[44] Thus, the predicted 2.5 kcal/mol difference in energy of the *endo* and *exo* transition states appears significant to the stereoselectivity.. A value of 2.7 kcal/mol was obtained earlier for the *endo*/*exo* transition state energy at a somewhat higher level of theory.[43] For the dimers, the lowest energy barrier **11** (29.3 kcal/mol) leads to dimer **10** for the most exothermic reaction. **10** is 33.6 kcal/mol lower in energy than two separated non-interacting monomers **9**. A similar trend may be observed in the energies of the products as was seen with the transition states. **10** is the most stable dimer and **7** the least, while **11** is the lowest and **8** the highest energy transition state.

These barriers probably are significantly larger than experiment as would be expected for *ab initio* SCF level predictions. For the dimerization of cyclopentadiene[43] the activation barrier for *endo* addition was 40.8 kcal/mol (HF/6-31(d)//HF/6-31G(d)), 5.4 kcal/mol (MP2/6-31(d)//HF/6-31G(d)), and 20.7 kcal/mol (MP3/6-31G(d)//HF/6-31G(d)). Thus, extending Møller–Plesset perturbation theory to third order was shown earlier to be important in comparison with experiment.[43] The experimental activation energy for the dimerization of cyclopentadiene has been measured to be between 14.9 and 16.9 kcal/mol in the gas phase[45,46] and between 15.9 and 17.7 kcal/mol[45,47] in solution. It has been shown theoretically[43] that the energies of the various minima or for that matter of the transition states relative to one another do not change substantially on moving from HF to the MP2 or MP3 levels of theory with a polarized basis set and using the HF/6-31G(d) geometries. For example,[43] the energy differences between the *endo* and *exo* transition states for cyclopentadiene itself are within 0.6 kcal/mol of each other (in kcal/mol): 2.6 (SCF/6-31G(d)//SCF/6-31G(d)), 3.2 (MP2/6-31G(d)//SCF/6-31G(d)), and 2.7 (MP3/6-31G(d)//SCF/6-31G(d)) at the various theoretical levels noted in brackets.

Which of the four possible 1-oxaspiro[2.4]hepta-4,6-diene adducts is predicted to form? There are four possible dimers of 1-oxaspiro[2.4]hepta-4,6-diene with barriers of 32.4 (**17**), 35.2 (**18**), 37.2 (**19**), and 39.6 kcal/mol (**20**) at the SCF level (see Figure 3 for the different isomers). If the lowest energy pathway is followed, the reaction barrier is predicted to be 32.4 kcal/mol (**17**) and the dimer minimum **13** is formed. 1-Oxaspiro[2.4]hepta-4,6-diene (**12**) was observed to dimerize quickly and spiro[2.4]hepta-4,6-diene (**6**) did not dimerize with an additional energy requirement that is predicted from theory to be approximately 13 kcal/mol. This predicted 13 kcal/mol difference in barrier heights is the quantification of the above-mentioned experimental observations regarding reactivity. One factor determining these reaction barriers may be a steric one given that it has been suggested previously that an oxygen is less sterically demanding.[48] The barrier to the dimerization of the cyclopentadiene systems can also be examined. The *endo* reaction barrier corresponding to transition state **3** is intermediate in comparison with those for **8** and **17**. Thus it would be

(44) Cristol, S. J.; Seifert, W. K.; Soloway, S. B. *J. Am. Chem. Soc.* **1960**, *82*, 2351.
(45) (a) Benford, G. A.; Wassermann, A. *J. Chem. Soc.* **1939**, 362. (b) Wassermann, A. *Monatsh. Chem.* **1952**, *83*, 543.
(46) (a) Khambata, B. S.; Wassermann, A. *Nature* **1937**, *139*, 669. (b) Harkness, J. B.; Kistiakowsky, G. B.; Mears, W. H. *J. Chem. Phys.* **1937**, *5*, 682. (c) Larkin, F. S.; Thrush, B. A. *Tenth Symposium on Combustion*; Combustion Institute: Pittsburgh, 1965; p 397. (d) Schumacker, H. J. *Chemische Gasreaktionen*; Steinkopf: Dresden, 1938; pp 256 and 301.
(47) (a) Sauer, J.; Wiest, H.; Mielert, A. *Chem. Ber.* **1964**, *97*, 3183. (b) Braun, R.; Schuster, F.; Sauer, J. *Tetrahedron Lett.* **1986**, *27*, 1285. (c) Keene, J. P. *Radiat. Res.* **1964**, *22*, 14. (d) Baxendale, J. H. *Radiat. Res.* **1962**, *17*, 312.
(48) Jones, P. G.; Weinmann, H.; Winterfeldt, E. *Angew. Chem., Int. Ed. Engl.* **1995**, *34*, 448.

Table 2. HOMO/LUMO Gaps for the Monomeric Cyclopentadiene (**1**), Spiro[2.4]hepta-4,6-diene (**6**), 1,2-Dioxaspiro[2.4]hepta-4,6-diene (**9**), and 1-Oxaspiro[2.4]hepta-4,6-diene (**12**)[a]

	HOMO	LUMO	gap
1	−0.310 90	0.133 18	12.08
6	−0.305 25	0.123 03	11.65
9	−0.345 86	0.073 33	11.41
12	−0.322 54	0.102 35	11.56

[a] Predictions were made on the fully optimized structures at the Hartree–Fock level using the 6-311G(d,p) basis set. The energies of HOMO and LUMO are in hartrees, and the HOMO/LUMO gaps are given in electronvolts.

expected that the rate of dimerization of cyclopentadiene would also be intermediate. The half-life of approximately 16 h at room temperature (toward dimerization) supports this analysis.

The HOMO-LUMO energy gaps for the four different systems with the 6−311G(d,p) basis set are given in Table 2. For the spiroheptadienes, this energy gap decreases from the all-carbon three-membered-ring to a single oxygen in the ring and on to two oxygens in the ring. The three-membered-ring substituents cause smaller HOMO-LUMO gaps. Net Mulliken charges on the spiro carbon are −0.37 (**1**), −0.07 (**6**), +0.25 (**12**), and +0.69 (**9**), and thus the electron-withdrawing nature of the substituents can be seen to decrease the HOMO/LUMO gap. Cyclopentadiene is somewhat anomalous relative to the substituted species as its larger HOMO-LUMO gap does not correlate with the intermediate (between 1-oxaspiro[2.4]hepta-4,6-diene and spiro[2.4]hepta-4,6-diene) predicted activation energies from the rigorous *ab initio* studies.

A frontier orbital analysis of the interactions begins with Figure 6, which shows computer-generated drawings of the HOMOs and LUMOs for the three spiroheptadienes. As can be seen, the HOMOs of the three systems change very little upon substitution. However, the basis functions on the substituents play a much larger role in the LUMOs. An antibonding interaction occurs between the substituents at C_3 and the π^* orbital across $C_2-C_3-C_4$ (see the arrow in Figure 6). This destabilizing interaction is less of a factor for the oxygen-containing compound (**9**) as the substituent orbital is both smaller and polarized away from the cyclopentyl ring. This interaction is fairly substantial as indicated by the coefficients in the LUMO. The LUMO basis function coefficients (at C_2 and C_4) are 0.269 (**6**), 0.259 (**12**), and 0.246 (**9**), while the substituent coefficients are −0.372 for **6**, −0.369 (C) and 0.179 (O) for **12**, and −0.168 for **9** (6-31G(d)). Clearly, the larger the coefficients on the substituents, the greater is the antibonding interaction, leading to destabilizations of the LUMOs. This analysis indicates that the oxygen substituents destabilize the LUMO less than the carbon substituents, thus leading to smaller HOMO-LUMO gaps for the oxygen-containing systems.

In this study only the *endo* isomers of the spiroheptadienes were examined. It is interesting that in the dimerization of cyclopentadiene, the *exo* product is predicted to be 1.2 kcal/mol more stable than the *endo*, but the *endo* transition state barrier is 2.5 kcal/mol lower than the *exo*. The bond angle at the two bond-forming carbons (see Figure 3: $C_3-C_4-C_{10}$ and $C_1-C_5-C_8$) for the *endo* and the *exo* minima can be compared. Clearly, the bond angles of 115.4° ($C_6-C_5-C_8$) and 115.8° ($C_3-C_4-C_{10}$) for the *exo* minimum are somewhat closer to the sp^3 hybridized value than are the respective *endo* bond angles of 118.0° and 118.3°. Slightly less strain in the *exo* minimum may be one reason why this minimum is 1.2 kcal/mol lower in energy than the *endo* minimum. However, in the transition state, it has been suggested[35] that secondary overlap effects are an

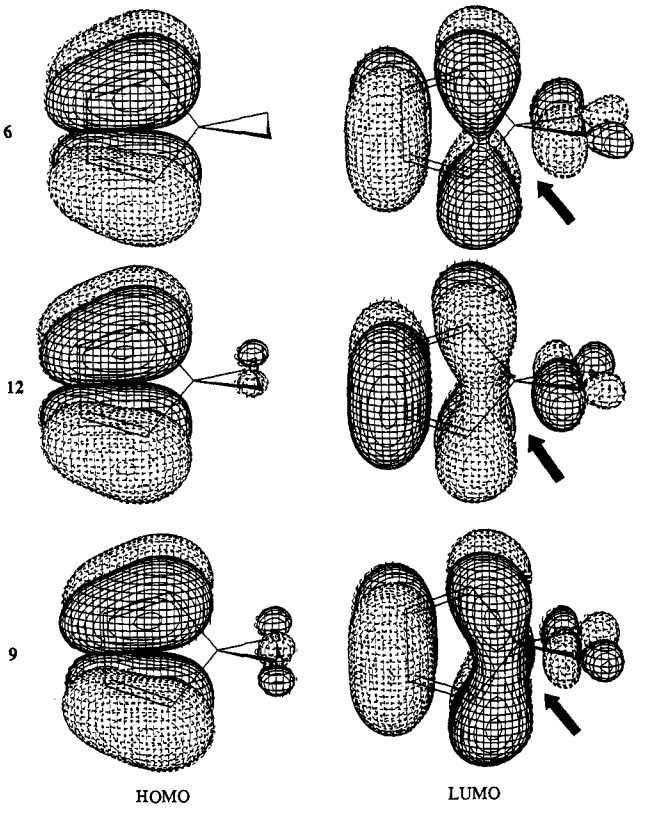

Figure 6. Plots of the HOMO and LUMO of the three substituted cyclopentadiene monomers, spiro[2.4]hepta-4,6-diene (**6**), 1-oxaspiro-[2.4]hepta-4,6-diene (**12**), and 1,2-dioxaspiro[2.4]hepta-4,6-diene (**9**). The SCF 6-31G(d) method was used. In each system, the node formed in the LUMO between the substituent basis functions and the π^* type orbital in the cyclopentadiene ring is emphasized by the arrow.

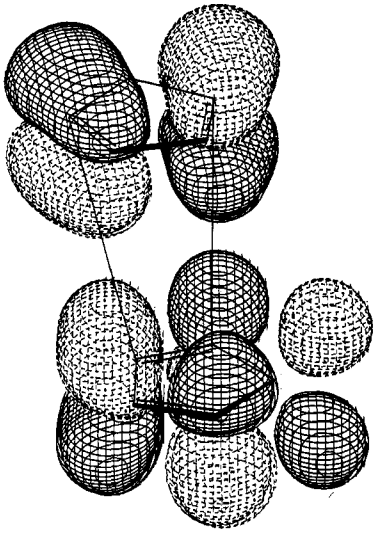

Figure 7. 6-31G(d) MO plots depicting the possible overlap between the HOMO of the diene (upper) and the LUMO of the dienophile (lower) of cyclopentadiene (**1**, *endo*). The bonds which are to be formed are indicated by the solid lines between the monomers.

important feature favoring *endo* additions. Figure 7, which shows the HOMO and LUMO superimposed, indicates how significant secondary orbital overlap could occur. The π-orbital of the diene interacts in an in-phase fashion with the π^*-orbital of the dienophile. These orbital diagrams further suggest that *endo* rather than *exo* products should be preferred.

(b) Geometries. The important bond lengths and bond angles for the four monomers at the SCF level with the 6-31G(d) basis set are given in Figure 1. The lengths of the two C−C bonds

which are formed in the transition states are shown in Figures 2 and 3. In addition, the 1-oxaspiro[2.4]hepta-4,6-diene dimer minimum (**13**) and the transition state (**17**) linking it to the two separated monomeric units (**12**) are shown in Figures 4 and 5 (SCF/6-31G(d)). The full geometries of the eleven other dimer minima and transition states are available in the supporting information in both Z-matrix and Cartesian coordinate form. The SCF 6-31G(d) optimized bond lengths for dimer **13** and for the methyl-substituted structure determined by X-ray crystallography are compared in Figure 4.

Cyclopentadiene has been examined before using *ab initio* methods.[49] The preferred geometries of the rings in various substituted cyclopentadienes are planar. Experimentally, the structure of cyclopentadiene is known[50] and is given in Figure 1. The predicted C_1-C_2, C_2-C_3, and C_1-C_5 bond lengths in the three spiroheptadiene systems (**6**, **9**, **12**) can be compared to those in cyclopentadiene as indicated in Figure 1.

There is only one possible *endo* adduct which can be formed from **1**, **6**, and **9**. However, for the adduct of 1-oxaspiro[2.4]-hepta-4,6-diene, there are four possible isomers. Reviewing the energetics of **7** and **10** can help predict which of these epoxide adducts might form. One can observe that dimer **10** with two oxygen substituents is much lower in energy in comparison to its monomers than the carbon/carbon analog **7** is with respect to **6**. Thus, the two oxygen substituents which point inward (see Figure 3) must be interacting more strongly and in a stabilizing manner in the product and in the transition state. Thus, it is not surprising that of the possible 1-oxaspiro[2.4]-hepta-4,6-diene dimer minima, the most stable species (**13**) has the oxygens directed inward (transition state **17** also has the lowest barrier). Transition state energetics can be explained using similar arguments. The minimum **16**, which has both carbons directed inward, is the least stable of the four isomers. The two 1-oxaspiro[2.4]hepta-4,6-dienes which have one oxygen inward and one outward in the diene and dienophile should be noted. One simple picture of the reaction involves the HOMO of the diene interacting with the LUMO of the dienophile. Thus a closer examination of the contribution of the substituents to the HOMO and the LUMO is necessary. There is almost no contribution to the HOMO (diene) by the substituents (see the molecular orbitals of the substituted monomers in Figure 6). There are considerable contributions to the LUMO of the dienophile. Thus, transition state **18** leading to dimer **14** where the oxygen of the dienophile is pointing inward (methylene outward) is predicted to be more stable than **15** where the oxygen of the diene is pointing inward (methylene outward). Our *ab initio* data predict that **14** is 1.6 kcal/mol more stable than **15**, and similarly that transition state **18** is 2.0 kcal/mol more stable than **19**. See Figure 3 for the structures of these transition states.

Figures 2 and 3 show the lengths of the two C−C bonds being formed in the seven different transition states. These fourteen bond lengths are 0.44 to 0.91 Å greater than in the product dimer. The lack of symmetry in the transition states may be correlated to the barrier height. The general trend is that the more unsymmetric the transition state, the smaller the barrier. As has been observed empirically earlier,[43] the sum of the lengths of the two bonds being formed is nearly constant. In the eight transition states considered in this work, the two bond lengths sum to 4.44 ± 0.04 Å. The two bond lengths in the various minima for each product are nearly equal although they differ markedly in the transition states as has been noted before.[5,7,8,51] It might be expected based on steric arguments and from earlier work on the butadiene/acrolein system[8] that of the two bonds being formed, the one at the more highly substituted end of the double bond of the dienophile would be longer. Therefore, in the present case, it might be suggested that the C_4-C_{10} distance would be greater than the C_5-C_8 distance. However, in all these dimerizations, the opposite order of bond lengths was observed. In the absence of any clearly steric argument, it is necessary to look for an electronic effect by examining the frontier orbitals of the various monomers.

The magnitudes of the coefficients of key basis functions in the HOMO of the diene and the LUMO of the dienophile were examined. The coefficients of importance (for the atom numbering, see Figure 1) are the HOMO coefficients for the functions on carbons 2 and 4 in the diene, which are identical (call them 2). These basis functions overlap with the LUMO in which the coefficients of the functions on carbons 1 and 2 or 4 and 5 in the dienophile are critical (call them 4 and 5). The basis function overlaps HOMO(C_2)-LUMO(C_4) and HOMO-(C_2)-LUMO(C_5) are important to bond formation at the transition state. Since the basis functions on C_2 in the HOMO are involved in both overlap terms, the strength of the bond being formed is dependent on the relative size of the coefficients of the basis functions in the LUMO at C_4 and the LUMO at C_5. In all three substituted cyclopentadienes, the coefficients of the basis functions are larger at carbon 4 than carbon 5, hence bonding is expected to be stronger at position 4. In each of the twelve cases, the bond length at C_4 is shorter than that at C_5. These bond length differences appear large given that the difference in the magnitude of the basis function coefficients is not that great. However, in the region of the cycloaddition transition state where the bonds being formed are still very weak and quite long, geometries can often change markedly with only small concomitant changes in energy. A similar analysis of basis function overlap indicated that, indeed, the longer bond length in the transition state in the addition of acrolein to butadiene should occur at the substituted end of the dienophile.

A comparison of the changes in the geometry from the monomer (**12**) to the transition state (**17**) and on to the dimer (**13**) will be made for the 1-oxaspiro[2.4]hepta-4,6-diene system (see Figures 1, 3, 4, and 5). In the monomer (**12**), the three bond lengths away from the ring substituent are 1.326 (C_4-C_5), 1.486 (C_1-C_5), and 1.326 Å (C_1-C_2). In the dienophile portion of the transition state structure, these bond lengths change to 1.333, 1.459, and 1.400 Å, which become 1.320, 1.506, and 1.562 Å, respectively, in the product dimer. As the predicted lengths indicate, one double bond is unaffected, whereas the other is transformed into a single bond. In the diene, the formally double bonds between C_6 and C_{10} and between C_7 and C_8 rearrange to one double bond between C_6 and C_7 (Figure 3). The transition state bond lengths for these three distances in the diene become 1.374, 1.400, and 1.398 Å, and the corresponding dimer bond lengths are 1.517, 1.324, and 1.517 Å, respectively.

(c) **Crystal Structure.** In the preparation of 1-oxaspiro[2.4]-hepta-4,6-diene, the species dimerized immediately. During this process, two isomers were formed in a 3:1 ratio. Similarly, two adducts were isolated when substituted monomers were the reactants. The major adduct of the substituted dimerization of 2,2-dimethyl-1-oxaspiro[2.4]hepta-4,6-diene was crystalline and an X-ray crystal structure analysis was carried out. The theoretically predicted unsubstituted dimer product, **13**, with

(49) (a) Boerth, D. W.; Morais, J. *J. Mol. Struct.* **1989**, *183*, 257. (b) Replogle, E. S.; Trucks, G. W.; Staley, S. W. *J. Phys. Chem.* **1991**, *95*, 6908.

(50) Damiani, D.; Ferretti, L.; Gallinella, E. *Chem. Phys. Lett.* **1976**, *37*, 265.

(51) Hancock, R. A.; Wood, B. F., Jr. *J. Chem. Soc., Chem. Commun.* **1988**, 351.

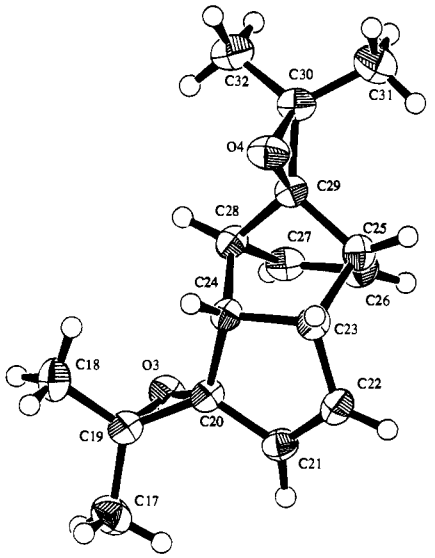

Figure 8. ORTEP drawing of the substituted dimer of the 1-oxaspiro-[2.4]hepta-4,6-diene species (**21**). This species corresponds to unsubstituted dimer **13**.

both oxygens pointing inward toward the newly formed bond, has the same conformation as the structure which has been examined via X-ray crystallography.

In the X-ray crystal structure of the dimer of 2,2-dimethyl-1-oxaspiro[2.4]hepta-4,6-diene, two independent molecules were found in the unit cell. For many important bond lengths and bond angles, the average absolute deviation between these two independent molecules was only 0.4%. The largest discrepancy is a CCO angle in the strained 3-membered ring where a 1.2% difference resulted from two distinct crystal structures having angles of 59.4° and 60.1°, respectively. In general, the largest differences between these two independent molecules are in the bond lengths and bond angles of the three-membered rings. Since the two independent molecules differed very little in their structures, a comparison with the theoretical geometries will be made with one of the two molecules. The ORTEP drawing of this species is given in Figure 8. The ORTEP drawing of the adduct (**21**) clearly indicates the *endo* nature of the product. Full details of the X-ray structure are available in the supporting information.

In comparing the SCF 6-31G(d) bond lengths shown in Figure 4 with the crystallographic data, once again the largest discrepancy, which is actually quite small, occurs for the three-membered rings. In comparing these values, the six exterior bond lengths (both the diene and dienophile) have an average absolute deviation from SCF theory of 2.8%, while the interior 12 bond lengths differ by on average only 0.5%. Thus, agreement between theory and experiment for the interior ring bond lengths is quite satisfactory. Similar statements may be made regarding the bond angles for which the data are available in the supporting information. To some extent, methyl substitution in the experiments may be affecting our comparisons of the bond lengths and bond angles for the three-membered rings. For example, the CO bond length is 1.402 Å in oxirane (SCF/6-31G(d)) but lengthens by 0.011 to 1.413 Å in tetramethyloxirane at the same level of theory.

Conclusions

In situ epoxidation of fulvene resulted in the formation of the epoxy monomer, which immediately underwent a Diels–Alder dimerization to form two adducts in a ratio of 3:1. The major product of dimerization of 6,6-dimethylfulvene (**21**) was crystalline and the X-ray crystallographic structure of this species agreed well with the 6-31G(d) SCF predicted geometry for the unsubstituted compound. Molecular orbital diagrams indicate that secondary orbital overlap leads to a preference for *endo* rather than *exo* addition. Transition state barriers (all *endo*) at the SCF/6-31G(d) level were predicted to decrease in the following order: spiro[2.4]hepta-4,6-diene > cyclopentadiene > 1-oxaspiro[2.4]hepta-4,6-diene > 1,2-dioxaspiro[2.4]hepta-4,6-diene. Given the experimental facts that spiro[2.4]hepta-4,6-diene does not dimerize and cyclopentadiene dimerizes slowly and the above ordering of transition state barriers, it is understandable that 1-oxaspiro[2.4]hepta-4,6-diene dimerizes quickly relative to the former molecules. The transition state structures are very unsymmetrical in these systems with the two forming bonds differing by as much as 0.47 Å in length.

Experimental Section

All reactions were run under an atmosphere of dry nitrogen unless otherwise indicated. Anhydrous solvents were transferred by oven-dried syringe or cannula. Flasks were flame dried under a stream of nitrogen. Tetrahydrofuran (THF) was distilled from sodium benzophenone ketyl.

Melting points were determined on a Thomas-Hoover melting point apparatus in open capillaries and are uncorrected. Infrared spectra were recorded on a Nicolet 205 spectrophotometer. Proton and carbon-13 (^{1}H, ^{13}C) nuclear magnetic resonance spectra were recorded using a Varian Gemini 200 (200 MHz, 50 MHz) or 300 (300 MHz, 75 MHz) spectrometer. Proton NMR spectra used for analytical determinations (e.g., product ratios) were run with an increased delay (0.5–1.0 s) to minimize effects of differential relaxation times.

1-Oxaspiro[2.4]hepta-4,6-diene Dimer (13). Fulvene was prepared *in situ* by dissolving 587 mg (4.77 mmol) of 5-((dimethylamino)-methyl)-1,3-cyclopentadiene[52] in 2.0 mL of dry THF at 0 °C followed by 297 μL (678 mg, 4.77 mmol) of CH_3I. After being stirred for 1 h, the solution appeared as a thick yellow slurry (because of the presence of the tetramethylammonium iodide salts) and was filtered through No. 1 Whatman filter paper using a Hirsh filter funnel and rinsed with the minimum amount of dry THF possible. The concentration of fulvene in the resultant solution was estimated to be 2 M based on the amount of 5-((dimethylamino)methyl)-1,3-cyclopentadiene used in the beginning and by analysis of the NMR spectrum of the filtrate (conversion appears to be >99%). The filtrate was cooled to −78 °C and to this was added the epoxidizing solution (also at −78 °C) which was prepared by adding 7.76 mL of *n*-butyl lithium (9.54 mmol, 1.23 M in hexanes) to 3.14 mL of *tert*-butyl hydroperoxide (11.9 mmol, 3.8 M in toluene) with no additional THF solvent used. The reaction temperature was allowed to come to −20 °C and was quenched by the addition of about 40 mg of solid Na_2SO_3 and stirring for 20 min. Five milliliters of H_2O was then added and the solution extracted into ether (3×), washed with brine, and dried over anhydrous $MgSO_4$. The crude product was then analyzed by ^{1}H NMR and two isomers were present in a ratio of 3:1. The ^{1}H NMR for the major isomer only is reported here: ^{1}H NMR (200 MHz, $CDCl_3$) δ 6.28 (m, 1H), 5.92 (m, 2H), 5.37 (dd, J = 5.6, 1.9 Hz, 1H), 3.67 (br t, J = 6 Hz, 3H), 3.14 (dd, J = 7.8, 4.2 Hz, 1H), 3.05 (d, J = 4.2 Hz, 1H), 2.97 (d, J = 4.2 Hz, 1H), 2.88 (m, 1H), 2.54 (m, 1H).

2,2-Dimethyl-1-oxaspiro[2.4]hepta-4,6-diene Adduct (21). Two hundred milligrams of **23** were dissolved in 0.5 mL of THF, the solution was cooled to −78 °C, and to this was added the epoxidizing solution (also at −78 °C). This solution was prepared by adding 1.69 mL of *n*-butyl lithium (2.08 mmol, 1.23 M in hexanes) to 0.75 mL of *tert*-butyl hydroperoxide (2.83 mmol, 3.8 M in toluene) which had been cooled to −78 °C. The reaction was allowed to come to room temperature and stirring was continued for 30 h at which point an additional 0.6 equiv of the oxidizing solution was added (after cooling back to −78 °C) as the reaction was only 60% complete and not progressing any further as judged by the NMR spectrum of the reaction mixture. After allowing the solution to warm to room temperature for

(52) Trost, B. M.; Cory, R. M. *J. Org. Chem.* **1972**, *37*, 1106.

8 h, the reaction was judged to be complete and was quenched by the addition of 40 mg of solid Na_2SO_3 and stirring for 20 min. Five milliliters of H_2O were then added and the solution extracted into ether (3×), washed with brine, and dried over anhydrous $MgSO_4$. The crude product was analyzed by NMR spectroscopy and its spectra showed the presence of two isomers in a ratio of 3:1. Pure major adduct could be obtained by crystallization (MeOH/H_2O) and spectral data are given below: mp 87 °C lit. mp (86−88 °C).[41b] ^{1}H NMR (200 MHz, $CDCl_3$) δ 6.20 (dd, J = 5.3, 3.3 Hz, 1H), 5.87 (m, 2H), 5.45 (dd, J = 5.8, 1.6 Hz, 1H), 3.54 (m, 1H), 3.00 (dd, J = 7.6, 4.6 Hz, 1H), 2.60 (br t, J = 4.2 Hz, 1H), 2.41 (br t, J = 4.4 Hz, 1H), 1.32 (s, 3H). ^{13}C NMR (200 MHz, $CDCl_3$, APT pulse sequence with C and CH_2 indicated by (+) and CH and CH_3 by (−)) δ 138.22 (−), 133.38 (−), 132.62 (−), 130.93 (−), 88.89 (+), 75.78 (+), 62.96 (+), 62.25 (+), 50.31 (−), 45.91 (−), 45.60 (−), 41.15 (−), 21.58 (−), 21.42 (−), 21.24 (−), 20.81 (−).

2,2-Cyclohexyl-1-oxaspiro[2.4]hepta-4,6-diene Dimer (25). Two hundred milligrams of **24** (1.37 mmol) were added to a 36 mol % solution of KOH (28 mg, 0.49 mmol) in 1 mL of MeOH at 0 °C. With strong stirring, 0.78 mL of H_2O_2 (30% solution, 6.58 mmol) was added dropwise as to keep the reaction temperature at 0 °C. The reaction was allowed to come to room temperature over 2 h at which point it was diluted with H_2O and extracted into ether (3×). The combined ether layers were treated with solid Na_2SO_3 (ca. 40 mg) which was washed out with one 5-mL rinse with H_2O. The ether layer was then rinsed once with brine and dried over anhydrous $MgSO_4$. Following solvent removal *in vacuo*, a crude NMR spectrum was taken which revealed the presence of two adducts in the ratio of 2:1. Based on crude weight, the two adducts gave a combined yield of approximately 70% with the remaining starting material accounting for the balance. Spectra of the major adduct are included here: ^{1}H NMR (200 MHz, $CDCl_3$) δ 6.25 (dd, J = 3.9, 2.0 Hz, 1H), 5.92−5.87 (m, 2H), 5.49 (dd, J = 3.3, 1.3 Hz, 1H), 3.60−3.54 (m, 1H), 3.00 (dd, J = 4.9, 3.3 Hz, 1H), 2.62 (br t, J = 1.6 Hz, 1H), 2.45 (br t, J = 1.6 Hz, 1H), 1.75−1.48 (m, 20H). ^{13}C NMR (200 MHz, $CDCl_3$, APT pulse sequence with C and CH_2 indicated by (+) and CH and CH_3 by (−)) δ 138.10 (−), 132.98 (−), 132.80 (−), 130.92 (−), 89.11 (+), 76.10 (+), 66.50 (+), 66.32 (+), 50.02 (−), 45.51 (−), 45.48 (−), 40.50 (−), 31.90 (+), 31.82 (+), 31.71 (+), 31.32 (+), 25.31 (+), 25.23 (+), 24.96 (+), 24.90 (+), 24.50 (+), 24.45 (+).

Theoretical Details. The Hartree−Fock method[53] within the GAUSSIAN 92 program[54] was used to predict the energies and geometries of the molecules. Minima and transition states were found using energy gradient methods and the algorithms of Schlegel.[55] Initially, small basis set STO-3G[56] geometry optimizations were carried out on the minima and transition states. The nature of these stationary points (minima and transition states) was characterized by determining the harmonic vibrational frequencies using analytic second-derivative[57] methods at the SCF level. For selected transition states, intrinsic reaction coordinates (IRC) were followed at the STO-3G SCF level in both the forward and reverse directions to ensure that the reactants and products were the expected separated monomers and the dimer. Then, higher level geometry optimizations of monomers, dimers, and transition states were carried out using the 6-31G(d) basis set.[58] The HOMO/LUMO gaps of the monomers were examined using the 6-311G(d,p) basis set.[58d,59] The PSI88 program[60] was used to plot the molecular orbitals determined with the 6-31G(d) basis set. Symmetry constraints were placed only on the monomers.

Acknowledgment. We thank Prof. Adrian Schwan for comments on an early draft of this manuscript. The Natural Sciences and Engineering Research Council of Canada (NSERC) are acknowledged for support in the form of a Postgraduate Scholarship (R.D.J.F.) and a Postdoctoral Fellowship (M.G.O.). J.D.G. acknowledges NSERC for support in the form of a Research Grant. The National Science Foundation is also acknowledged (B.M.T.).

Supporting Information Available: Tables of data from the crystallographic structure determination of **21** include crystal data, data collection conditions, solution and refinement details, positional parameters, anisotropic thermal factors, bond lengths, bond angles, torsional angles, collection data, and ORTEP drawings and SCF optimized geometries tabulated in Z-matrix and Cartesian coordinate (standard orientation) (40 pages). This material is contained in many libraries on microfiche, immediately follows this article in the microfilm version of the journal, can be ordered from the ACS, and can be downloaded from the Internet; see any current masthead page for ordering information and Internet access instructions.

JA951689O

(53) (a) Hartree, D. R. *Proc. Cambridge Phil. Soc.* **1928**, *24*, 89, 111, 246. (b) Fock, V. *Z. Phys.* **1930**, *61*, 126. (c) Roothaan, C. C. J. *Rev. Mod. Phys.* **1951**, *23*, 69.

(54) Gaussian 92, Revision B, Frisch, M. J.; Trucks, G. W.; Head-Gordon, M.; Gill, P. M. W.; Wong, M. W.; Foresman, J. B.; Johnson, B. G.; Schlegel, H. B.; Robb, M. A.; Replogle, E. S.; Gomperts, R.; Andres, J. L.; Raghavachari, K.; Binkley, J. S.; Gonzalez, C.; Martin, R. L.; Fox, D. J.; Defrees, D. J.; Baker, J.; Stewart, J. J. P.; Pople, J. A. Gaussian, Inc.: Pittsburgh, PA, 1992.

(55) Schlegel, H. B. *J. Comput. Chem.* **1982**, *3*, 214.

(56) Hehre, W. J.; Stewart, R. F.; Pople, J. A. *J. Chem. Phys.* **1969**, *51*, 2657.

(57) Pople, J. A.; Krishnan, R.; Schlegel, H. B.; Binkley, J. S. *Int. J. Quantum Chem. Symp.* **1979**, *13*, 225.

(58) (a) Hehre, W. J.; Ditchfield, R.; Pople, J. A. *J. Chem. Phys.* **1972**, *56*, 2257. (b) Francl, M. M.; Pietro, W. J.; Hehre, W. J.; Binkley, J. S.; Gordon, M. S.; DeFrees, D. J.; Pople, J. A. *J. Chem. Phys.* **1982**, *77*, 3654. (c) Hariharan, P. C.; Pople, J. A. *Theor. Chim. Acta* **1973**, *28*, 213. (d) Hariharan, P. C.; Pople, J. A. *Chem. Phys. Lett.* **1972**, *16*, 217.

(59) (a) Krishnan, R.; Binkley, J. S.; Seeger, R.; Pople, J. A. *J. Chem. Phys.* **1980**, *72*, 650. (b) McLean, A. D.; Chandler, G. S. *J. Chem. Phys.* **1980**, *72*, 5639. (c) Krishnan, R.; Frisch, M. J.; Pople, J. A. *J. Chem. Phys.* **1980**, *72*, 4244.

(60) Jorgensen, W. L.; Severance, D. L. Unpublished extended version of PSI/77. Jorgensen, W. L. *QCPE* **1980**, *12*, program 340.